Asian Journal of Chemistry; Vol. 34, No. 9 (2022), 2191-2197

ASIAN JOURNAL OF CHEMISTRY

https://doi.org/10.14233/ajchem.2022.23691

Pulmonary Phospholipid Components as Promising Natural Inhibitors against COVID-19 M^{pro}; Molecular Docking Analysis Based Study

MOHAMMED A. HUSSEIN[1,*], HEBA M. ABO-SALEM[2], AHMED M. MORO[3], EBTSAM A. ABDEL-WAHAB[3], ALI A ALI[4] and SHAIMAA A. ABDELKAWY[1]

[1]Department of Biotechnology, Faculty of Applied Health Sciences Technology, October 6 University, Sixth of October City, Egypt
[2]Department of Chemistry and Natural Compounds, Pharmaceutical and Drug industries Research Division, National Research Center, Dokki, Giza, Egypt
[3]Department of Biophysics, Faculty of Applied Medical Sciences, October 6 University, Sixth of October City, Egypt
[4]Department of Food Science, Faculty of Agriculture, Ain Shams University, Cairo, Egypt

*Corresponding author: Tel: +20 12 4832580; E-mail: prof.husseinma@o6u.edu.eg

Received: 21 December 2021; *Accepted*: 10 April 2022; *Published online*: 19 August 2022; AJC-20908

The ongoing pandemic of COVID-19 caused by the severe acute respiratory syndrome SARS-CoV-2 has become a global crisis. Phospholipids are structural components of mammalian cell membranes that suppress viral attachment to the plasma membrane and subsequent replication in lung cells. Using the molecular docking approach, the inhibitory activity of phosphatidylcholine, dipalmitoylphosphatidylcholine, phosphatidylethanolamine, phosphatidylglycerol, phosphatidyl-inositol, lysobisphosphatidic acid and sphingomyelin against SARS CoV-2 by targeting main protease (M^{pro}, PDB code: 6LU7) has been investigated. All phospholipids established excellent binding to M^{pro} active bocket by forming several H-bonds with the catalytic amino acids Cys145 and His4, as well as various amino acids involved in the bocket. Furthermore, a potent binding affinity is increased from -7.01 to -9.16 kcal/mol compared to compound **N3** (*N*-[(5-methylisoxazol-3-yl)carbonyl]alanyl-L (where L = valyl-N-1-(1*R*,2*Z*)-4-(benzyloxy)-4-oxo-1-{[(3R)-2-oxopyrrolidin-3-yl]methyl}but-2-enyl)-L-leucinamide), a peptide linker, inhibitor for Covid-19 main protease. Co-crystalline ligand of enzyme 6LU7 of -9.99 kcal/mol. The sphingomyelin has the same binding affinity to main protease when compared to compound **N3**. These findings implied that the selected compounds have the potential to be developed as novel SARS-CoV-2 inhibitors. Therefore, improved, well-designed, potent and structurally and pharmacokinetically effective drugs are urgently needed. Further investigations should focus on validating and finalizing effective drugs for COVID-19 beyond preliminary *in silico* and *in vivo* screening.

Keywords: Dipalmitoylphosphatidyl choline, Phosphatidyl glycerol, Lysobisphosphatidic acid, Sphingomyelin, SARS CoV-2, Protease.

INTRODUCTION

Most of the patients with mild to moderate breathing problems COVID-19 infection will recover without specific treatment [1]. Furthermore, COVID-19 represents a spectrum of clinical severity that ranged from asymptomatic to critical pneumonia, acute respiratory distress syndrome (ARDS) and even death [2]. Accumulating evidence suggests that the inflammatory mediators play a crucial role in COVID-19 [3,4]. Inflammatory responses caused by SARS-CoV-2 replication led to cell destruction and macrophages, as well as cytokine release [5].

Phospholipids are the most common molecular species that decrease inflammatory responses by interacting directly with certain cell receptors [5,6]. *in vitro*, the anionic phosphatidylglycerol and phosphatidylcholine contribute to alveolar surfactant dynamic activities [7,8]. Surfactants comprise 5-12% phosphatidylcholine, but lung tissue and other organ secretions are considerably enriched in this molecule [9-11]. In contrast, all mammalian surfactants investigated so far contain significant amounts of phosphatidylcholine, which are not prominent in other organs [12-15].

According to the early compositional investigations, dipalmitoyl phosphatidylcholine is the single most abundant component [16,17]. The capacity of interfacial coatings of lung surfactant to reduce surface tension to very low values during dynamic compression is probably certainly due to this disaturated phospholipid [18,19].

Several studies have established the role of intracellular phosphatidylinositol isoforms signalling in lung surfactant secreting epithelial type II cells and alveolar macrophages [20,21]. The expression of phosphatidylinositol b and g isoforms has been linked to the stimulation of differentiation and lung surfactant secretion in type II cells [22,23]. It is also involved in macrophage phagocytosis [24] and lung epithelial protection from oxidative stress generated by iNOS, inhibiting the amplification and continuation of an uncontrolled, oxidant-driven inflammatory cascade [25]. The abundance of phosphatidylethanolamine varies in the membranes of different tissues and cells in mammals and organelles of both yeast and mammals [26-28]. Recently, disturbances in phosphatidylethanolamine metabolism have been implicated in both chronic and infectious disease [29-32].

Sphingomyelins are found in the membranes of most of the eukaryotic cells [33]. Sphingomyelin accounts for 2-15% of total organ phospholipid in mammalian tissues, although specific tissues, such as the brain, peripheral nerve tissue and ocular lenses, have significantly greater sphingomyelin levels [34-36]. It emerges as a key molecule in the production of bioactive sphingolipids *via* ceramide. Sphingomyelin synthase is an enzyme that converts phosphatidylcholine and ceramide into sphingomyelin and diacylglycerol [37,38].

Several investigations have shown that under COVID-19 infections and its oxidative stress, phospholipids can be altered, leading to oxidized phospholipids. Influenza viruses and SARS-CoV [39,40] can induce pulmonary oxidized phospholipids accumulation, which is associated with a pro-inflammatory response, acute injury and organ damage [41]. Accumulation of oxPLs during COVID-19 infections, play a central role in induction of inflammatory responses and production ROS [42]. There are many reports showing that administration of exogenous surfactant and cytosolic phospholipase A2α inhibitors may help COVID-19 infected patients with chronic diseases [43,44]. The possible links between cellular phospholipid fractions metabolism in human metabolic diseases and the likelihood for a poor outcome following a COVID-19 infection are so far not fully understood. As a continuation of our research programme to explain the relation between COVID-19 infection and autoimmune response to alleviate the adverse antiviral activity of cellular phospholipid fractions against COVID-19 infection [43,44]. The goal of the present strategy is to use a molecular docking approach to evaluate the ability of lung phospholipid fractions (phosphatidylcholine, dipalmitoyl phosphatidylcholine, phosphatidylethanolamine, phosphatidylglycerol, phosphatidylinositol, lysobisphosph-atidic acid and sphingomyelin) to act as inhibitors for SARS CoV-2 main protease M^{pro} to be used in the COVID 19 treatment.

EXPERIMENTAL

Target preparation: The crystal structure of SARS-CoV-2 main protease in association with an inhibitor (*N*-[(5-methylisoxazol-3-yl)carbonyl]alanyl-L (where L = valyl-N-1-(1*R*,2*Z*)-4-(benzyloxy)-4-oxo-1-{[(3*R*)-2-oxopyrrolidin-3-yl]methyl}-but-2-enyl)-L-leucinamide) (**N3**) was retrieved from the protein data bank at http://www.rscb.org./pdb using 6LU7 codes [45]. The water molecules were removed and the enzyme was prepared using QuickPrep tool module in MOE 2019.01 (Molecular Operating Environment, Version 2019.01, Chemical Computing Group Inc., Montreal, Canada), then active site was identified.

The chemical structure of phosphatidylcholine, dipalmitoylphosphatidylcholine, phosphatidylethanolamine, phosphatidylglycerol, phosphatidylinositol, lysobisphosphatidic acid and sphingomyelin were obtained from ZINC database (https://zinc.docking.org/) or PubChem (https://pubchem.ncbi.nlm.nih.gov/) as sdf files then loaded to MOE program. The structures were minimized using the MMFF94x force field until the RMSD of 0.01 kcal mol^{-1} $Å^{-1}$ was reached. The induced-fit protocol was used in the docking simulation, with the Triangle Matcher method used to place ligand conformations in the site, which were then ranked using the London DG scoring function. The docking protocol was validated by running docking for the target protein's co-crystallized ligand. The re-docked ligand had a low RMSD value 1.47 $Å^{-1}$, indicating that the protocol was valid. For each compound, one hundred docking poses were calculated and the resulting docking poses were visualized using MOE 2019.01. The top-scored docking poses were used to calculate the binding free energy (DG) of compounds and co-crystallized ligand in kcal/mol.

RESULTS AND DISCUSSION

In present work, the inhibition activity of phosphatidylcholine, dipalmitoylphosphatidylcholine, phosphatidylethanolamine, phosphatidylglycerol, phosphatidylinositol, lysobisphosphatidic acid and sphingomyelin against SARS CoV-2 main protease M^{pro} were predicted utilizing the molecular docking technique. The high-resolution crystal structure of CoV-2-SARS main protease M^{pro} (PDB ID: 6LU7) in complex with the inhibitor **N3** was used in docking process.

The binding affinity and interaction manners of the selected compounds with the M^{pro} are shown in Table-1. First, the co-crystalline ligand, **N3** was re-docked into the active site to validate docking protocol. The re-docked ligand had binding affinity of -9.99 kcal/mol, formed seven H-bond donor with CYS 145, GLU 166, two H-bond acceptors GLU 166, GLN 189, four arene-H interactions with HIS 41 and a low RMSD value 1.47 $Å^{-1}$, which indicating that our protocol was valid (Fig. 1). While, phosphatidylcholine revealed excellent binding affinity of -8.75 kcal/mol in comparison to **N3** of -9.99 kcal/mol and formed powerful interaction with the enzyme active site through formation of five H-bond donors with CYS 145, GLU 166, ASN 142, eight H-bond acceptors with His 136, GLY 143 and six H-pi interaction with HIS 41, TYR 118 amino acid residues (Fig. 2). Dipalmitoylphosphatidylcholine displayed potent binding affinity of -8.93 kcal/mol in comparison to **N3** of -9.99 kcal/mol and established multiple hydrogen bonds with the M^{pro} active site as follow; six hydrogen bond donors with catalytic CYS 145, MET 49, MET 165, two H-acceptor with HIS 41, beside H-pi interaction with HIS 41 (Fig. 3). Furthermore, phosphatidylethanolamine showed docking score of -8.37 kcal/mol with formation of two H-bond donors with CYS 145, MET 49 and three H-bond acceptors with ASN 142 (Fig. 4). Moreover, the phosphatidylglycerol showed lowest

TABLE-1
MOLECULAR DOCKING RESULT OF PHOSPHOLIPID COMPOUNDS WITH THE SARS CoV-2 MAIN PROTEASE (PDB ID: 6LU7)

Comp. No.	Score (Kcal/mol)	Moieties from the compound	Amino acid residues	Type of interaction, Distance (Å)
N3	-9.99	CH_2	CYS 145	H-donor 3.53
		NH	THR 190	Two H-donor 2.85
		NH, CO	GLU 166	Two H-donor 2.84, Two H-acceptor 2.89
		NH	GLN 189	Two H-donor 3.00, 3.26
		CH_2, CH_3	HIS 41	Four Pi-H 4.04, 4.06, 4.22, 4.25
Phosphatidylcholine (ZINC8437505)	-8.75	OCH_2	CYS 145	Two H-donor 4.08
		O	GLU 166	H-donor 3.52; Ionic 3.93, 4.00
		O	ASN 142	H-donor 3.05, 2.99, 3.01
		CH_2, O	HIS 163	H-acceptor 3.57, 3.56
		CH_2	TYR 118	H-pi, 3.99, 4.01
		O	HIS 163	H-acceptor 3.33, 3.22, 3.21
		O	GLY 143	Three H-acceptor 2.89
		CH_2	HIS 41	H-pi 3.68, 3.62, 3.74, 4.29
Dipalmitoylphosphatidyl-choline (ZINC8214373)	-8.93	OH, O	CYS 145	H-donor 3.43, 3.55
		CH_2	MET 49	H-donor 4.14, 4.17
		CH_3	MET 165	H-donor 4.09, 4.05
		O	HIS 41	H-acceptor 3.46, 3.37
		CH_3	HIS 41	H-pi 3.58
Phosphatidylethanolamine (ZINC32793026)	-8.37	OH	CYS 145	H-donor 3.27, 3.32
		CO	MET 49	H-donor 4.34
		CH	ASN 142	Three H-acceptor 3.49
Phosphatidylglycerol (ZINC8552309)	-8.96	CO	CYS 145	H-donor 3.42, 3.52
		O	MET 165	H-donor 3.50
		OH	GLN 189	H-donor 2.52, 2.49, 2.74
		CH_2, CO	MET 165	H-donor 3.96, 3.94, 3.98
		CO	HIS 41	H-acceptor 3.32, 3.19, 3.25
Phosphatidylinositol (CID_9547150)	-8.50	OH	CYS 145	H-donor 3.38, 3.32, 3.33
		O H	MET 49	H-donor 4.12, 4.05, 4.05
		OH	GLU 166	H-donor 3.49,
		OH	GLU 166	Three H-acceptor 3.16
		O, OH	HIS 164	Three H-donor 2.87
Lysobisphosphatidic acid (CID_5497152)	-7.01	OH, CH_2	CYS 145	H-donor 3.72, 3.71, 3.97
		OH	GLU 166	H-donor 2.68, 2.67, 2.79, 4.01
		OH	ASN 142	H-donor 3.28, 2.97
		CH_2	HIS 41	H-acceptor 3.19
Sphingomyelin (ZINC8860498)	-9.16	O	CYS 145	H-donor 3.33, 3.35, 3.26, 3.18, 3.20
		NH	GLU 166	Ionic 3.79
		O	HIS 164	Three H-donor 3.06
		O	HIS 41	H-acceptor 3.28, 3.29
		N H	HIS 41	H-pi 4.55, 4.43, 4.46

binding energy of -8.96 kcal/mol and displayed excellent binding mode *via* formation of twelve hydrogen bonds with the active site in a good distance, nine H-donors with CYS 145, MET 165, GLN 189 and three H-acceptors with HIS 41 (Fig. 5). Phosphati-dylinositol revealed binding energy of -8.50 kcal/mol and established ten H-bond donors with CYS 145, MET 49, GLU 166, HIS 164 and three H-bond acceptors with GLU 166 (Fig. 6). On the other hand, lysobisphosphatidic revealed the binding energy of -7.01 kcal/mol and formed seven H-bond donors with CYS145, GLU 166, ASN 142 and one H-acceptor with HIS 41 (Fig. 7). Finally, sphingomyelin displayed the best binding affinity of -9.16 kcal/mol in comparison to **N3** of -9.99 kcal/mol, with excellent binding to the M^{pro} active site through establishment eight H-bond donors with CYS 145, HIS 164, two H-bond acceptors with HIS 41, in addition to three H-pi interaction with HIS 41 and Ionic interaction with GLU 166 (Fig. 8).

The main M^{pro} is relatively conserved and is what most drug repurposing studies are focusing [46,47]. However, viral evolution could change the structure of the M^{pro} substrate-binding pocket by causing mutations at the substrate-binding site and/or other locations. Surface loops and helical domains III, for example, vary between M^{pros} affecting the active site's conformation [48,49].

It's also important to consider the size of functional groups when building better medications because it affects drug binding modes on M^{pro}'s catalytic sites [50]. Several medication classes have been found to be effective against SARS-CoV-2 M^{pro}. Among the well-studied drug families are, peptide- and anilid-based inhibitors, medicines from Chinese traditional medicine, phytochemicals and indole lactam-based inhibitors. Although the FDA has approved remdesivir for the treatment of COVID-19 patients, its clinical efficacy is still in question [51-53]. Also, evaluation of plasma phospholipids as a neutral

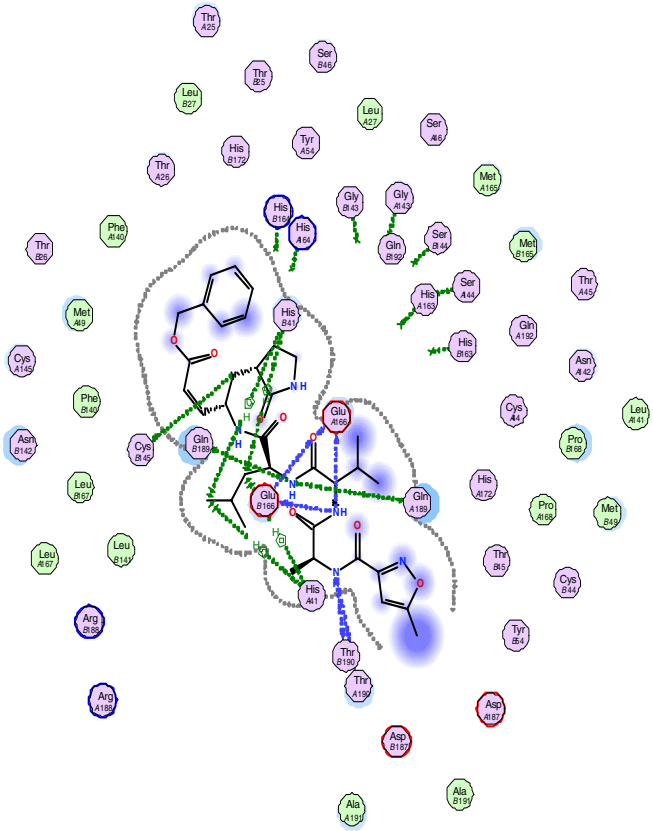

Fig. 1a. 2D interaction of co-crystalline ligand **N3** with the binding site of SARS CoV-2 main protease (PDB ID: 6LU7)

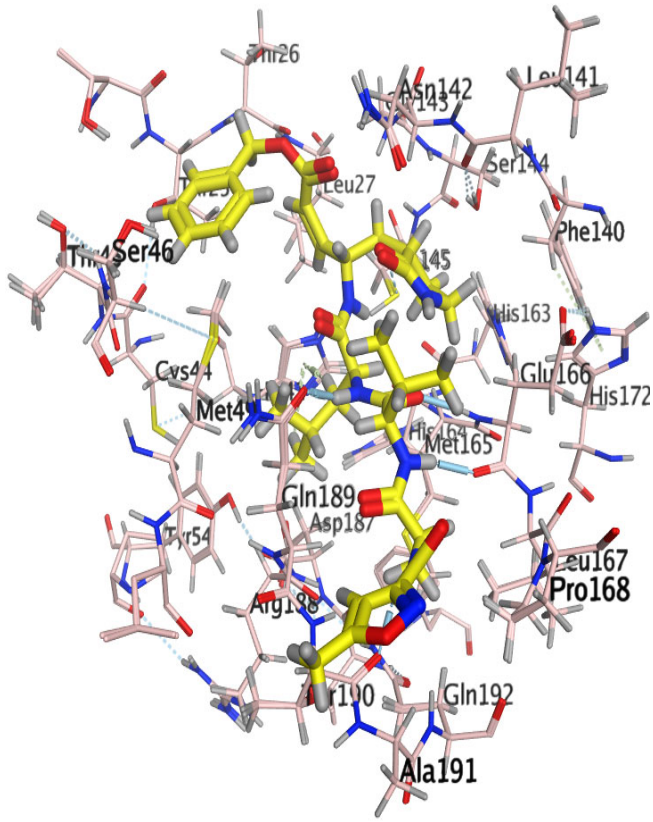

Fig. 1b. 3D interaction of **N3** with the binding site of SARS CoV-2 main protease (PDB ID: 6LU7)

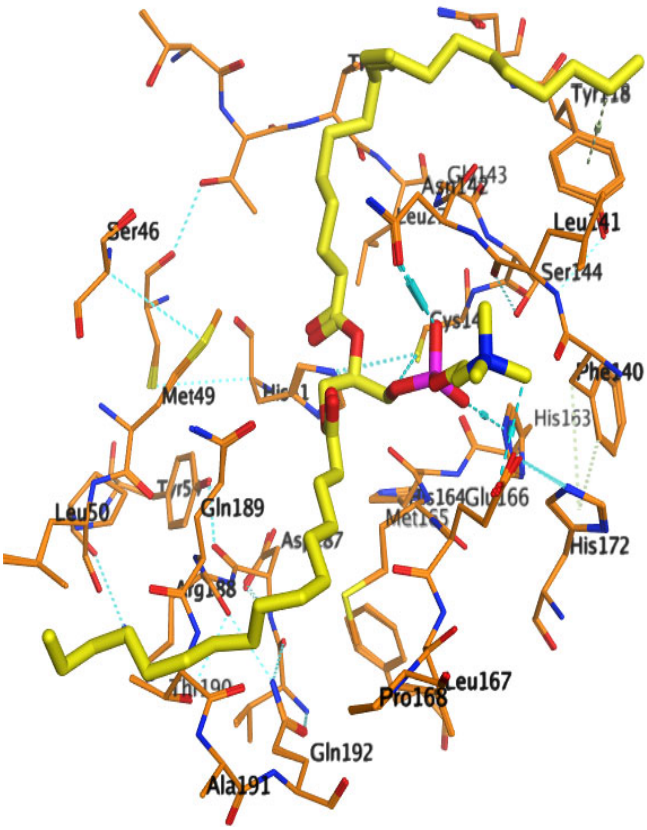

Fig. 2. 3D interaction of phosphatidylcholine (yellow stick) with the binding site of SARS CoV-2 main protease (PDB ID: 6LU7)

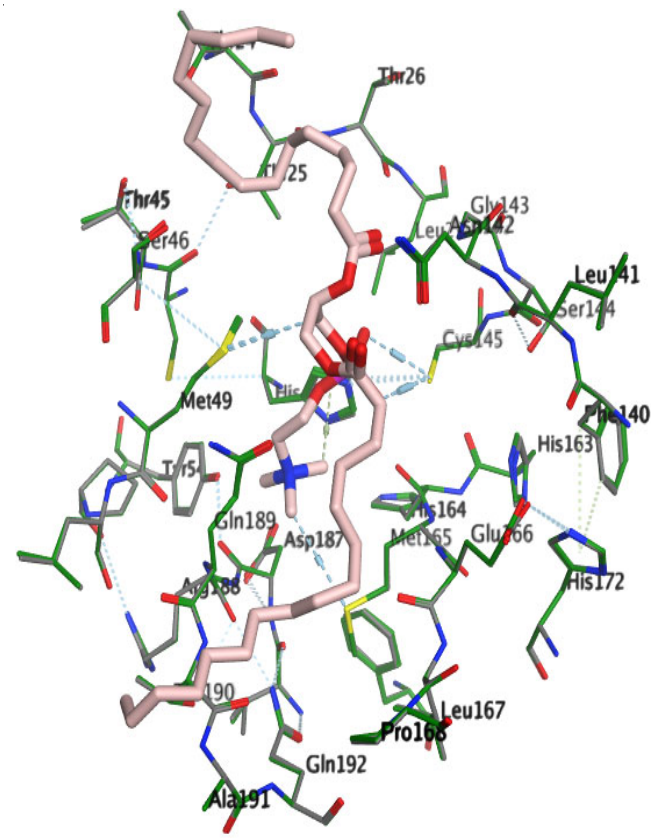

Fig. 3. 3D interaction of dipalmitoylphosphatidylcholine (pink stick) with the binding site of SARS CoV-2 main protease (PDB ID: 6LU7)

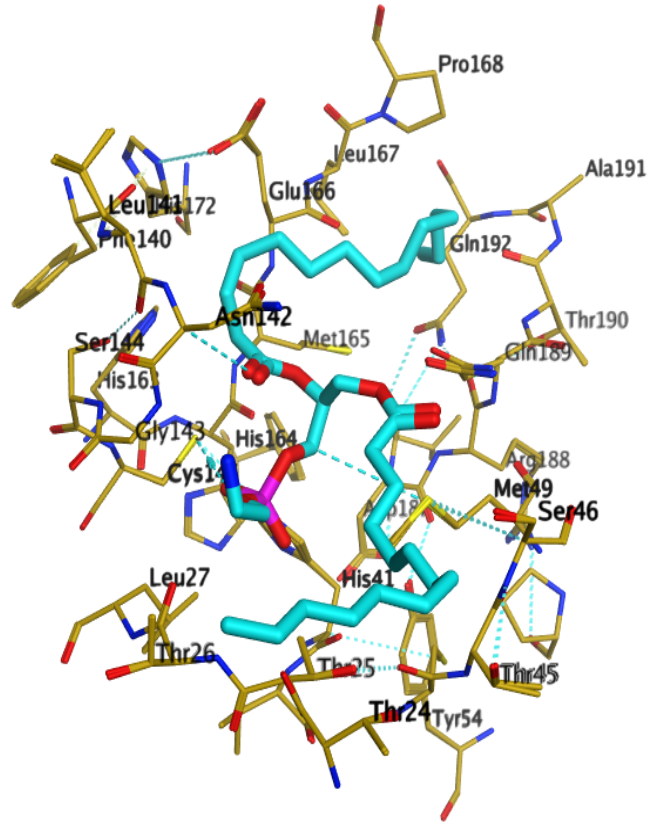

Fig. 4. 3D interaction of phosphatidylethanolamine (cyan stick) with the binding site of SARS CoV-2 main protease (PDB ID: 6LU7)

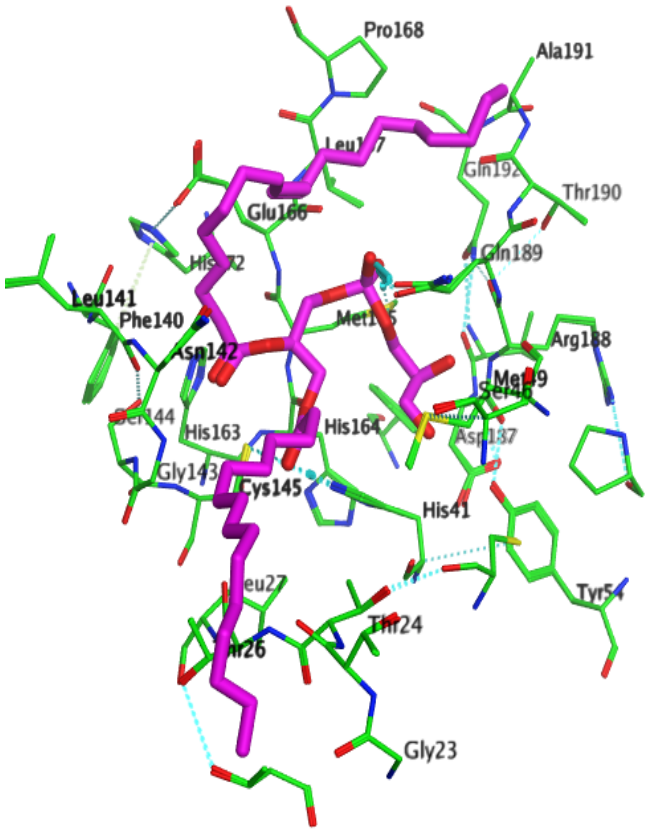

Fig. 5. 3D interaction of phosphatidylglycerol (purple stick) with the binding site of SARS CoV-2 main protease (PDB ID: 6LU7)

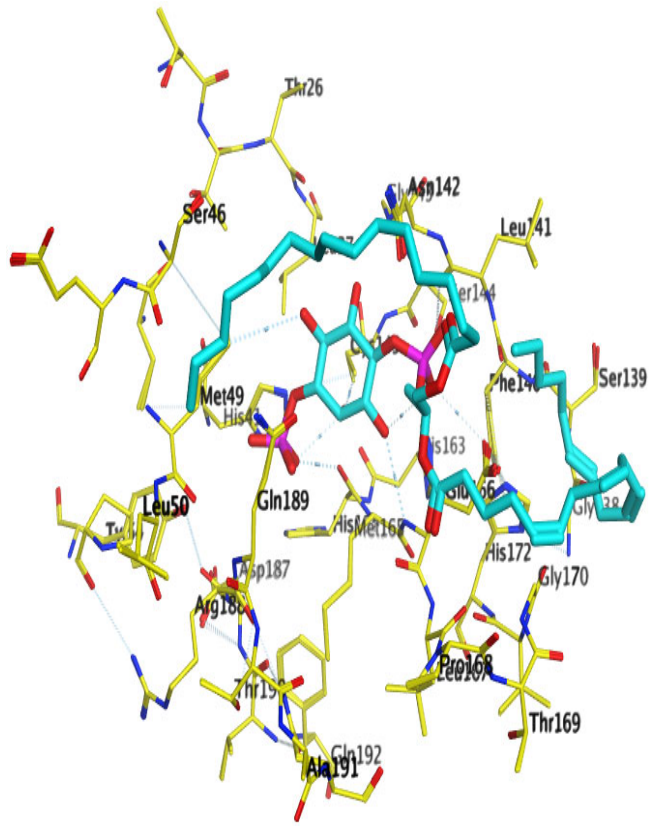

Fig. 6. 3D interaction of phosphatidylinositol (green stick) with the binding site of SARS CoV-2 main protease (PDB ID: 6LU7).

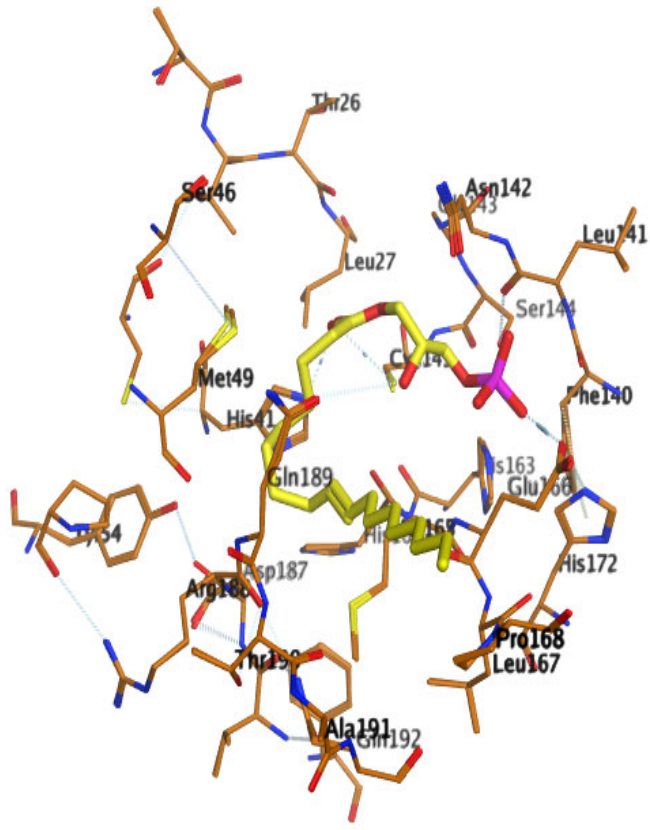

Fig. 7. 3D interaction of lysobisphosphatidic (yellow stick) with the binding site of SARS CoV-2 main protease (PDB ID: 6LU7)

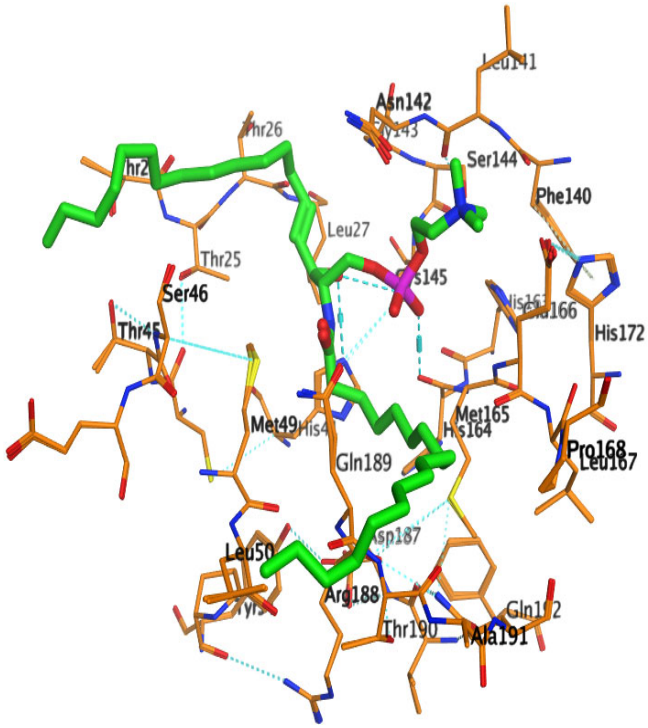

Fig. 8. 3D interaction of sphingomyelin (green stick) with the binding site of SARS CoV-2 main protease (PDB ID: 6LU7)

inhibitors against SARS-CoV-2 M^{pro} has not been reported earlier to our best of knowledge and this study is perhaps the first observation of its kind.

Conclusion

In current study, the molecular docking technique was used to describe the ability of phosphatidylcholine, dipalmitoylphosphatidylcholine, phosphatidylethanolamine, phosphatidylglycerol, phosphatidylinositol, lysobisphosphatidic acid and sphingomyelin to act as SARS-CoV-2 main protease inhibitors. Overall results proposed that all studied compounds had potent binding affinity from -7.01 to -9.16 kcal/mol in comparison to **N3** of -9.99 kcal/mol. All compounds interacted well with the SARS-CoV-2 M^{pro} active bocket, forming multiple H-bonds with the two catalytic amino acids CYS 145 and HIS 41, as well as several amino acids in the bocket. As a result, the investigated compounds can be candidates for *in vitro* testing against SARS-COV-2 main protease and, as a result, the inhibition of replication of SARS-COV2 responsible for pandemic COVID-19.

CONFLICT OF INTEREST

The authors declare that there is no conflict of interests regarding the publication of this article.

REFERENCES

1. H. Lu, C.W. Stratton and Y.W. Tang, *J. Med. Virol.*, **92**, 401 (2020); https://doi.org/10.1002/jmv.25678
2. G. Lippi and M. Plebani, *Clin. Chim. Acta*, **505**, 190 (2020); https://doi.org/10.1016/j.cca.2020.03.004
3. P. Mehta, D.F. McAuley, M. Brown, E. Sanchez, R.S. Tattersall and J.J. Manson, *Lancet*, **395**, 1033 (2020); https://doi.org/10.1016/S0140-6736(20)30628-0
4. J. Stebbing, A. Phelan, I. Griffin, C. Tucker, O. Oechsle, D. Smith and P. Richardson, *Lancet Infect. Dis.*, **20**, 400 (2020); https://doi.org/10.1016/S1473-3099(20)30132-8
5. M.Z. Tay, C.M. Poh, L. Renia, P.A. MacAry and L.F.P. Ng, *Nat. Rev. Immunol.*, **20**, 363 (2020); https://doi.org/10.1038/s41577-020-0311-8
6. S. Akpinar, M. Oran, M. Dogan, A. Çelikkol, I. Erdem and B. Turgut, *Eur. Rev. Med. Pharmacol. Sci.*, **25**, 5304 (2021); https://doi.org/10.26355/eurrev_202108_26551
7. O.V. Oskolkova, V. Godschachner and V.N. Bochkov, *Inflammation*, **40**, 530 (2017); https://doi.org/10.1007/s10753-016-0499-8
8. S. Karnati, V. Garikapati, G. Liebisch, P.P. Van Veldhoven, B. Spengler, G. Schmitz and E. Baumgart-Vogt, *PLoS One*, **13**, e0203464 (2018); https://doi.org/10.1371/journal.pone.0203464
9. S.N. Nguyen, J.E. Kyle, S.E. Dautel, R. Sontag, T. Luders, R. Corley, C. Ansong, J. Carson and J. Laskin, *Anal. Chem.*, **91**, 11629 (2019); https://doi.org/10.1021/acs.analchem.9b02045
10. W. Bernhard, *Ann. Anat.*, **208**, 146 (2016); https://doi.org/10.1016/j.aanat.2016.08.003
11. S.A. Boshra and M.A. Hussein, *Int. J. Phytomed.*, **8**, 217 (2016).
12. W. Stremmel, R. Ehehalt, S. Staffer, S. Stoffels, A. Mohr, M. Karner and A. Braun, *Dig. Dis.*, **30(Suppl. 3)**, 85 (2012); https://doi.org/10.1159/000342729
13. T. Becker, G. Loch, M. Beyer, I. Zinke, A.C. Aschenbrenner, P. Carrera, T. Inhester, J. Schultze and M. Hoch, *Nature*, **463**, 369 (2010); https://doi.org/10.1038/nature08698
14. W. Stremmel, *Z. Gastroenterol.*, **51**, 384 (2013); https://doi.org/10.1055/s-0033-1335042
15. W. Stremmel, A. Hanemann, A. Braun, S. Stoffels, M. Karner, S. Fazeli and R. Ehehalt, *Expert Opin. Investig. Drugs*, **19**, 1623 (2010); https://doi.org/10.1517/13543784.2010.535514
16. I. Bersani, C.P. Speer and S. Kunzmann, *Expert Rev. Anti Infect. Ther.*, **10**, 573 (2012); https://doi.org/10.1586/eri.12.34
17. S.R. Bates, *Cell. Physiol. Biochem.*, **25**, 41 (2010); https://doi.org/10.1159/000272062
18. M.X. Rojas-Reyes, C.J. Morley and R. Soll, *Cochrane Database Syst. Rev.*, **3**, CD000510 (2012); https://doi.org/10.1002/14651858.CD000510.pub2
19. M.S. Dunn, J. Kaempf, A. de Klerk, R. de Klerk, M. Reilly, D. Howard, K. Ferrelli, J. O'Conor and R.F. Soll, *Pediatrics*, **128**, e1069 (2011); https://doi.org/10.1542/peds.2010-3848
20. N. Seger and R. Soll, *Cochrane Database Syst. Rev.*, **2**, CD007836 (2009); https://doi.org/10.1002/14651858.CD007836
21. A. Hamvas, *Chin. Med. J. (Engl.)*, **123**, 2943 (2010).
22. T.H. Garmany, J.A. Wambach, H.B. Heins, J.M. Watkins-Torry, D.J. Wegner, K. Bennet, P. An, G. Land, O.D. Saugstad, H. Henderson, L.M. Nogee, F.S. Cole and A. Hamvas, *Pediatr. Res.*, **63**, 645 (2008); https://doi.org/10.1203/PDR.0b013e31816fdbeb
23. V. Boggaram, *Clin. Sci.*, **116**, 27 (2009); https://doi.org/10.1042/CS20080068
24. R.M. DiBlasi and I.M. Cheifetz, *Respir. Care*, **56**, 1466 (2011); https://doi.org/10.4187/respcare.01505
25. J.E. Vance, *Biochim. Biophys. Acta*, **1841**, 595 (2014); https://doi.org/10.1016/j.bbalip.2013.11.014
26. J.E. Vance, *Traffic*, **16**, 1 (2015); https://doi.org/10.1111/tra.12230
27. K.S. Dimmer and D. Rapaport, *Biochim. Biophys. Acta Mol. Cell Biol. Lipids*, **1862**, 69 (2017); https://doi.org/10.1016/j.bbalip.2016.07.010
28. T. Tatsuta and T. Langer, *Biochim. Biophys. Acta Mol. Cell Biol. Lipids*, **1862**, 81 (2017); https://doi.org/10.1016/j.bbalip.2016.08.006
29. M.G. Acoba, N. Senoo and S.M. Claypool, *J. Cell Biol.*, **219**, e202003131 (2020); https://doi.org/10.1083/jcb.202003131
30. J.Y. Choi, M.T. Duraisingh, M. Marti, C. Ben Mamoun and D.R. Voelker, *J. Biol. Chem.*, **290**, 10972 (2015); https://doi.org/10.1074/jbc.M115.642413

31. J.-Y. Choi, Y. Augagneur, C.B. Mamoun and D.R. Voelker, *J. Biol. Chem.*, **287**, 222 (2012); https://doi.org/10.1074/jbc.M111.313676
32. N.R. Deleault, J.R. Piro, D.J. Walsh, F. Wang, J. Ma, J.C. Geoghegan and S. Supattapone, *Proc. Natl. Acad. Sci. USA*, **109**, 8546 (2012); https://doi.org/10.1073/pnas.1204498109
33. G. D'Angelo, S. Moorthi and C. Luberto, *Adv. Cancer Res.*, **140**, 61 (2018); https://doi.org/10.1016/bs.acr.2018.04.009
34. Z. Li, T.K. Hailemariam, H. Zhou, Y. Li, D.C. Duckworth, D.A. Peake, Y. Zhang, M.S. Kuo, G. Cao and X.C. Jiang, *Biochim. Biophys. Acta*, **1771**, 1186 (2007); https://doi.org/10.1016/j.bbalip.2007.05.007
35. T. Ding, Z. Li, T. Hailemariam, S. Mukherjee, F.R. Maxfield, M.-P. Wu and X.-C. Jiang, *J. Lipid Res.*, **49**, 376 (2008); https://doi.org/10.1194/jlr.M700401-JLR200
36. L. Hua, N. Wu, R. Zhao, X. He, Q. Liu, X. Li, Z. He, L. Yu and N. Yan, *Int. J. Mol. Sci.*, **20**, 2861 (2019); https://doi.org/10.3390/ijms20122861
37. X. Li, T. Luo, H. Li and N. Yan, *Molecules*, **25**, 4231 (2020); https://doi.org/10.3390/molecules25184231
38. Y. Chen and Y. Cao, *Biol. Chem.*, **398**, 1319 (2017); https://doi.org/10.1515/hsz-2017-0148
39. H.A. El-Gizawy and M.A. Hussein, *Int. J. Phytomed.*, **7**, 219 (2015).
40. N.A.E.K. Gobba, A.A. Hussein, D.E. El Sharawy and M.A. Hussein, *Arch. Environ. Occup. Health*, **73**, 189 (2018); https://doi.org/10.1080/19338244.2017.1314930
41. M. Leppkes, J. Knopf, E. Naschberger, A. Lindemann, J. Singh, I. Herrmann, M. Stürzl, L. Staats, A. Mahajan, C. Schauer, A.N. Kremer, S. Völkl, K. Amann, K. Evert, C. Falkeis, A. Wehrfritz, R.J. Rieker, A. Hartmann, A.E. Kremer, M.F. Neurath, L.E. Muñoz, G. Schett and M. Herrmann, *EBioMedicine*, **58**, 102925 (2020); https://doi.org/10.1016/j.ebiom.2020.102925
42. B. Gallo Marin, G. Aghagoli, K. Lavine, L. Yang, E.J. Siff, S.S. Chiang, T.P. Salazar-Mather, L. Dumenco, M.C. Savaria, S.N. Aung, T. Flanigan and I.C. Michelow, *Rev. Med. Virol.*, **31**, 1 (2021); https://doi.org/10.1002/rmv.2146
43. M.A. Hussein, *Coronaviruses*, **2**, Article ID: e080921192222 (2021); https://doi.org/10.2174/2666796702666210311123323
44. M.A. Hussein, N.E.M. Ismail, A.H. Mohamed, R.M. Borik, A.A. Ali and Y.O. Mosaad, *Bioinform. Biol. Insights*, **15**, 11779322211055891 (2021); https://doi.org/10.1177/11779322211055891
45. Z. Jin, X. Du, Y. Xu, Y. Deng, M. Liu, Y. Zhao, B. Zhang, X. Li, L. Zhang, C. Peng, Y. Duan, J. Yu, L. Wang, K. Yang, F. Liu, R. Jiang, X. Yang, T. You, X. Liu, X. Yang, F. Bai, H. Liu, X. Liu, L.W. Guddat, W. Xu, G. Xiao, C. Qin, Z. Shi, H. Jiang, Z. Rao and H. Yang, *Nature*, **582**, 289 (2020); https://doi.org/10.1038/s41586-020-2223-y
46. S. Ullrich and C. Nitsche, *Bioorg. Med. Chem. Lett.*, **30**, 127377 (2020); https://doi.org/10.1016/j.bmcl.2020.127377
47. P. Eleftheriou, D. Amanatidou, A. Petrou and A. Geronikaki, *Molecules*, **25**, 2529 (2020); https://doi.org/10.3390/molecules25112529
48. K. Akaji and H. Konno, *Molecules*, **25**, 3920 (2020); https://doi.org/10.3390/molecules25173920
49. T. Mohammad, A. Shamsi, S. Anwar, M. Umair, A. Hussain, M.T. Rehman, M.F. AlAjmi, A. Islam and M.I. Hassan, *Virus Res.*, **288**, 198102 (2020); https://doi.org/10.1016/j.virusres.2020.198102
50. B. Goyal and D. Goyal, *ACS Comb. Sci.*, **22**, 297 (2020); https://doi.org/10.1021/acscombsci.0c00058
51. M.L. Holshue, C. DeBolt, S. Lindquist, K.H. Lofy, J. Wiesman, H. Bruce, C. Spitters, K. Ericson, S. Wilkerson, A. Tural, G. Diaz, A. Cohn, L. Fox, A. Patel, S.I. Gerber, L. Kim, S. Tong, X. Lu, S. Lindstrom, M.A. Pallansch, W.C. Weldon, H.M. Biggs, T.M. Uyeki and S.K. Pillai, *N. Engl. J. Med.*, **382**, 929 (2020); https://doi.org/10.1056/NEJMoa2001191
52. Y. Wang, D. Zhang, G. Du, R. Du, J. Zhao, Y. Jin, S. Fu, L. Gao, Z. Cheng, Q. Lu, Y. Hu, G. Luo, K. Wang, Y. Lu, H. Li, S. Wang, S. Ruan, C. Yang, C. Mei, Y. Wang, D. Ding, F. Wu, X. Tang, X. Ye, Y. Ye, B. Liu, J. Yang, W. Yin, A. Wang, G. Fan, F. Zhou, Z. Liu, X. Gu, J. Xu, L. Shang, Y. Zhang, L. Cao, T. Guo, Y. Wan, H. Qin, Y. Jiang, T. Jaki, F.G. Hayden, P.W. Horby, B. Cao and C. Wang, *Lancet*, **395**, 1569 (2020); https://doi.org/10.1016/S0140-6736(20)31022-9
53. J.D. Norrie, *Lancet*, **395**, 1525 (2020); https://doi.org/10.1016/S0140-6736(20)31023-0